

Protonmotive force regulates the membrane conductance of *Streptococcus bovis* in a non-ohmic fashion

Daniel R. Bond¹ and James B. Russell^{1,2}

Author for correspondence: J. B. Russell. Tel: +1 607 255 4508. Fax: +1 607 255 3904.
e-mail: jbr8@cornell.edu

Section of Microbiology,
Cornell University¹, and
Agricultural Research
Service, USDA², Ithaca,
NY 14853, USA

Because the DCCD (dicyclohexylcarbodiimide)-sensitive, F-ATPase-mediated, futile ATP hydrolysis of non-growing *Streptococcus bovis* JB1 cells was not affected by sodium or potassium, ATP hydrolysis appeared to be dependent only upon the rate of proton flux across the cell membrane. However, available estimates of bacterial proton conductance were too low to account for the rate of ATP turnover observed in *S. bovis*. When de-energized cells were subjected to large pH gradients (2.75 units, or –170 mV), internal pH declined at a rate of 0.15 pH units s⁻¹. Based on an estimated cellular buffering capacity of 200 nmol H⁺ (mg protein)⁻¹ per pH unit, H⁺ flux across the cell membrane (at –170 mV) was 108 mmol (g protein)⁻¹ h⁻¹. When potassium-loaded cells were treated with valinomycin in low-potassium buffers, initial K⁺ efflux generated membrane potentials in close agreement with values predicted by the Nernst equation. These artificial membrane potentials drove H⁺ uptake, and H⁺ influx was counterbalanced by a further loss of cellular K⁺. Flame photometry indicated that the rate of K⁺ loss was 215 (±26) mmol K⁺ (g protein)⁻¹ h⁻¹ at –170 mV, but the potassium-sensitive fluorescent compound CD222 indicated that this rate was only 110 (±44) mmol K⁺ (g protein)⁻¹ h⁻¹. As pH gradients or membrane potentials were reduced, the rate of H⁺ flux declined in a non-ohmic fashion, and all rates were <25 mmol (g protein)⁻¹ h⁻¹ at a driving force of –80 mV. Previous estimates of bacterial proton flux were based on low and unphysiological protonmotive forces, and the assumption that H⁺ influx rate would be ohmic. Rates of H⁺ influx into *S. bovis* cells [as high as 9 × 10⁻¹¹ mol H⁺ (cm membrane)⁻² s⁻¹] were similar to rates reported for respiring mitochondria, but were at least 20-fold greater than any rate previously reported in lactic acid bacteria.

Keywords: protonmotive force, proton conductance, energy spilling, *Streptococcus bovis*

INTRODUCTION

Non-growing bacteria often consume energy sources at a rapid rate (frequently termed ‘resting’, ‘energized’ or ‘glycolysing’ cells), and these bacteria have multiple strategies of becoming less efficient when energy is in excess. Excess energy can be stored as cellular polymers

(e.g. glycogen or polyhydroxybutyrate), but these pools are quickly saturated. Energy sources can be diverted through fermentation or respiratory pathways that generate less ATP, but some bacteria utilize futile cycles to regenerate ADP so metabolism can continue (Taylor & Jackson, 1987; Neijssel & Teixeira de Mattos, 1994; Russell & Cook, 1995).

Non-growing *Streptococcus bovis* ferments sugars at a rate that greatly exceeds its needs for maintenance, lacks alternative respiratory pathways, does not store polymers, and only uses substrate-level phosphorylation to generate ATP (Russell & Strobel, 1990).

Abbreviations: 9-AA, 9-aminoacridine; BCECF, 2,7-bis(2-carboxyethyl)-5(6)-carboxyfluorescein; BCECF-AM, acetoxymethyl ester derivative of BCECF; DCCD, dicyclohexylcarbodiimide; TCS, tetrachlorosalicylanilide; TPP, tetraphenylphosphonium.

Because non-growth ATP hydrolysis could be strongly inhibited by the F-type ATPase inhibitor DCCD (dicyclohexylcarbodiimide) and was stimulated by protonophores, it appeared that *S. bovis* was using a proton-pumping F-ATPase to turn over excess ATP. Similar observations have been made in *Enterococcus* (Harold & Baarda, 1969) and *Lactococcus* (Maloney, 1977).

Previous work indicated that changes in intracellular inorganic phosphate could play a role in regulation of ATP hydrolysis in *S. bovis*. When energy was in excess, inorganic phosphate decreased, the ΔG° of ATP hydrolysis was greater, and protonmotive force generated by the F-ATPase was significantly higher (Bond & Russell, 1998). Gross estimates based on Ohm's law indicated that the resistance of the cell membrane to protons declined as protonmotive force increased, allowing faster rates of ATP hydrolysis and proton pumping. However, proton flux rates predicted by these calculations were 20–50-fold faster than values previously measured in bacteria (Maloney, 1979; Rius & Lorén, 1998; Rius *et al.*, 1994; Bender *et al.*, 1986).

The following experiments with *S. bovis* sought to: (1) generate artificial protonmotive forces similar to those observed in fermenting cells, (2) investigate the relationship between protonmotive force and ion flux, and (3) compare these fluxes to other biological systems.

METHODS

Cell growth. *Streptococcus bovis* JB1 was routinely grown under O₂-free CO₂ at 39 °C in basal medium containing (per litre): 2 g glucose, 292 mg K₂HPO₄, 292 mg KH₂PO₄, 480 mg (NH₄)₂SO₄, 480 mg NaCl, 100 mg MgSO₄·7H₂O, 64 mg CaCl₂·2H₂O, 500 mg cysteine hydrochloride, 1 g Trypticase (BBL Microbiology Systems), 4 g Na₂CO₃ and 0.5 g yeast extract. The medium was adjusted to pH 6.7 and the final pH was never less than 6.5.

Glucose consumption rate of non-growing cells. Starved cells (>4 h in stationary phase to deplete intracellular potassium) were washed three times (10000 g, 5 min, 4 °C) in anoxic buffer (100 mM MES/HCl, 0.5 mM MgCl₂ and 3 mM cysteine, prepared with double-distilled H₂O, pH 6.8), resuspended to a final concentration of 240 µg protein ml⁻¹, gassed with a continuous stream of O₂-free N₂ in a temperature-controlled chamber (39 °C) and provided with 8 mg glucose ml⁻¹. NaCl or KCl (5 mM), valinomycin (1 µM) or tetrachlorosalicylanilide (TCS; 1 µM) was added where indicated. Glucose consumption by non-growing cells was measured by monitoring bacterial heat production as described previously (Russell & Strobel, 1990) with an LKB 2277 Bioactivity monitor equipped with semi-conducting Peltier elements as thermopiles and gold flow cells. The instrument was calibrated with an internal heat source, and the flow cell was sterilized with 95% ethanol and 1 M HCl. The flow cell temperature was set at 39.00 °C. The glucose consumption rate was estimated from the enthalpy (ΔH) of glucose conversion to lactate [87.6 J (mmol glucose)⁻¹] and the conversion factor 0.278 mW J⁻¹ h⁻¹. As 2 ATP are produced per glucose fermented, non-growing cells must hydrolyse 2 ATP per glucose for glucose consumption to continue.

Intracellular pH measurements using BCECF. The hydrophilic

compound 2,7'-bis(2-carboxyethyl)-5(6)-carboxyfluorescein (BCECF) was purchased as its hydrophobic acetoxyethyl ester derivative (BCECF-AM) (Molecular Probes). *S. bovis* cells were grown to stationary phase, washed three times in buffer (10 mM K₂HPO₄, 80 mM KCl, 0.5 mM MgCl₂ and 0.5 mM DTT, pH 7.8), concentrated 20-fold and equilibrated/de-energized for 12 h (22 °C) with 0.1 µM valinomycin. After equilibration, cells were centrifuged, resuspended in 0.5 ml of the same buffer, and BCECF-AM was added to a final concentration of 10 µM (from a concentrated stock dissolved in DMSO). BCECF-AM can diffuse into cells and be cleaved by intracellular esterases, and BCECF is trapped inside cells. The fluorescence of BCECF is pH-dependent, and this compound can serve as an indicator of intracellular pH. Cells were incubated with BCECF-AM for 1 h at 39 °C, washed twice with 40 ml of buffer containing 0.1 µM valinomycin, resuspended to a final optical density of approximately 100 (600 nm, 1 cm light path), and stored on ice until use. The presence of valinomycin and excess potassium ions allowed for charge compensation when protons entered cells during the assay (Maloney, 1977). If valinomycin was omitted, proton influx rates were significantly inhibited. Cells were diluted 100-fold into 39 °C buffer containing 0.1 µM valinomycin, and equilibrated for 15 s in 3 ml cuvettes in a Bio-Rad VersaFluor fluorimeter (490 nm excitation, 520 nm emission). Extracellular pH was lowered by adding 5–40 µl 1 M HCl while vigorously stirring the cuvette with a pipette. Measurements could reliably be recorded within 5–6 s of acid addition. Extracellular pH was determined in the cuvette 30 s after acid addition, with a pH meter. DCCD-treated cells were incubated in 1 mM DCCD for 30 min before being assayed in buffer containing 0.5 mM DCCD. Intracellular pH was calibrated for each batch of cells by adding 1 mM each valinomycin and nigericin, adding HCl, and recording both fluorimeter readings and pH in the cuvette. Cell suspensions were not subjected to more than five readings during calibration, to minimize photobleaching. Calibrations performed after loading and 2 h later gave similar results, indicating that leakage (efflux) of the probe (Molenaar *et al.*, 1991, 1992) was not significant.

Measurement of proton flux using 9-aminoacridine (9-AA).

As the neutral form of the fluorescent amine 9-AA can freely cross the cell membrane, the distribution of 9-AA (inside versus outside) is pH-dependent. Because only extracellular 9-AA gives fluorescence, uptake and quenching of 9-AA fluorescence is an indicator of decreased intracellular pH (Casadio *et al.*, 1995). Potassium-loaded cells were obtained by harvesting cells during growth, and washing them three times in 4 °C choline buffer (50 mM choline chloride, 10 mM Bistris, 0.5 mM MgCl₂, 0.5 mM DTT, prepared with double-distilled H₂O, pH 6.8). Cells were concentrated to an OD₆₀₀ of approximately 100 and kept on ice until use. Warmed buffer (39 °C) containing 0.4 µM 9-AA was placed in pre-warmed acid-washed glass vials, cells were added to a final concentration of 1.5 OD₆₀₀ units (0.9 mg protein ml⁻¹), and the vial was placed in a Perkin Elmer model 203 fluorescence spectrophotometer (405 nm excitation, 495 nm emission) to obtain a baseline. Unless otherwise stated, 0.1 µM valinomycin was added to establish a membrane potential. Measurements could be obtained within 5 s of closing the instrument door, and quenching of 9-AA was measured over the next 30 s. Rates of proton influx were estimated from the initial rate (first 10% of quenching). Potassium (as KCl) was added to vials to adjust membrane potential, and membrane potentials were calculated using the Nernst equation. Previous work indicated that more than 98% of intracellular potassium in *S. bovis* is

unbound (Strobel & Russell, 1989). Intracellular [typically 1.5 mmol K^+ (g protein^{-1}), or approx. 350 mM] and extracellular (typically $0.2\text{--}0.4 \text{ mM}$ unless otherwise adjusted) potassium concentrations were measured by flame photometry as described below (9-AA did not interfere with flame photometry). DCCD treatment was the same as for BCECF-loaded cells.

Measurement of intracellular potassium efflux using flame photometry. Potassium-loaded cells were prepared from growing cells as described for 9-AA-based measurements. Choline buffer (1 ml , 39°C) with added potassium to reduce the membrane potential was placed in pre-warmed acid-washed glass tubes with stir bars. Concentrated cell suspensions were added and allowed to equilibrate for 30 s at 39°C (final concentration $0.2\text{--}0.4 \text{ mg protein ml}^{-1}$). Valinomycin was added, and cells were centrifuged through silicone oil at various times. Sampling times were from the time of valinomycin addition to the initiation of centrifugation. Samples ($100 \mu\text{l}$) of supernatant were removed, the tubes were frozen, and once the liquid above the silicone was solid, cell pellets were removed with dog nail-clippers. Supernatants and cell pellets were digested at room temperature for 24 h in 3 M HNO_3 , and insoluble cell debris was removed by centrifugation (10000 g , 15 min). The potassium concentration was determined by flame photometry (Cole-Parmer 2655-00 Digital Flame Analyzer, Cole-Parmer Instrument Co.).

When the filter method was employed, lower cell densities ($0.1 \text{ mg protein ml}^{-1}$) were utilized so cells could be rapidly separated from supernatant. Valinomycin was added to the cell suspensions (1 ml), potassium efflux was terminated with the addition of 2 ml ice-cold 100 mM LiCl , and cell suspensions were immediately filtered through Millipore type HA $0.45 \mu\text{m}$ filters that had been pre-soaked in 100 mM LiCl . The filter was then rinsed with an additional 2 ml of cold LiCl to remove contaminating potassium from the filter. Filters were digested in 3 M HNO_3 for 24 h , and analysed as described. Duplicate samples were centrifuged through silicone oil to obtain supernatant samples for extracellular potassium determination.

Measurement of potassium efflux using CD222. Potassium-loaded cells were washed and concentrated in choline buffer and placed in pre-warmed, acid-washed glass vials ($0.24 \text{ mg protein ml}^{-1}$). CD222 ($1 \mu\text{M}$), a fluorescent probe sensitive to extracellular potassium (Molecular Probes), was added to the cell suspensions, and preliminary results found CD222 to be sensitive in the range of $0.05\text{--}1.0 \text{ mM}$ potassium. After a baseline was obtained (Perkin Elmer model 203 fluorescence spectrophotometer; 365 nm excitation, 465 nm emission), $0.1 \mu\text{M}$ valinomycin was added, and the increase in fluorescence was monitored. Measurements could be obtained within 5 s of closing the instrument door. Potassium efflux rates were based on the difference between extracellular potassium at time of valinomycin addition and the concentration 10 s later. The system was calibrated by adding potassium (up to 1.5 mM) directly to vials containing cells and using flame photometry to determine the initial extracellular potassium concentrations (typically $0.4\text{--}0.6 \text{ mM}$). Membrane potentials were adjusted by adding extracellular potassium (to 1 mM) or by using cells that had only been allowed to partially deplete their intracellular potassium. Potassium-depleted cells were washed in buffer to remove residual potassium before use.

ATPase activity of inverted vesicles. Membrane vesicles were prepared as previously described (Russell *et al.* 1988). Briefly,

10 ml of lysozyme/mutanolysin-treated protoplasts were rapidly diluted in 1 litre of low-osmotic-strength buffer, incubated with DNase and RNase, unbroken cells removed by low-speed centrifugation (1000 g , 30 min , 4°C), and vesicles were harvested by high-speed centrifugation (30000 g , 30 min , 4°C). This vesicle preparation was washed twice in buffer (50 mM potassium phosphate, $\text{pH } 7.0$, 10 mM MgSO_4), concentrated to $24.5 \text{ mg protein ml}^{-1}$, and passed twice through a French pressure cell at 55 MPa . Inverted vesicles were washed twice in buffer (35000 g , 30 min , 4°C), and concentrated to $14 \text{ mg protein ml}^{-1}$. Some inverted vesicles were assayed for ATPase activity the same day, and the rest were frozen at -80°C . Freezing for up to 3 d did not significantly affect ATPase activity.

ATPase activity was assayed by a method employing pyruvate kinase as described by Bond & Russell (1996). The assay contained (per ml): $10\text{--}20 \text{ mg}$ liposome protein, $50 \mu\text{mol}$ triethanolamine, $2 \mu\text{mol MgCl}_2$, $0.16 \mu\text{mol NADH}$, $0.83 \mu\text{mol}$ phosphoenolpyruvate, and 5 units each pyruvate kinase and lactate dehydrogenase ($\text{pH } 7.0$, 39°C). DCCD addition only reduced the ATPase activity $50\text{--}70\%$, but pre-incubation of inverted vesicles with DCCD (15 min , 1 mM) eliminated 90% of the activity. The ATPase activity of inverted vesicles and whole cells was normalized using the assumption that 15% of cell protein is associated with the membrane (Maloney, 1987; Cramer & Knaff, 1991). Protein was measured by the Lowry method after boiling vesicles in 0.2 M NaOH .

Other assays. Membrane potential was estimated from the uptake of $[^3\text{H}]\text{TPP}^+$. Cells were incubated with $[^3\text{H}]\text{TPP}^+$ (10 nM , $851 \text{ GBq mmol}^{-1}$; Amersham) for 2 min (or shorter intervals, if indicated). The cells were centrifuged through silicone oil, and $[^3\text{H}]\text{TPP}^+$ in pellets and supernatants was measured by scintillation counting. Cells were de-energized for 10 min with $10 \mu\text{M}$ valinomycin and $10 \mu\text{M}$ nigericin to correct for nonspecific $[^3\text{H}]\text{TPP}^+$ binding, and separate determinations of nonspecific binding were made for each potassium concentration or medium condition (Lolkema *et al.*, 1982). $[^{14}\text{C}]\text{Benzoate}$ ($1 \mu\text{M}$ final concentration, $0.81 \text{ GBq mmol}^{-1}$; Amersham) was used in a similar fashion to determine intracellular pH of glycolysing cells. The intracellular volume of whole cells was assumed to be $4.3 \mu\text{l}$ (mg protein^{-1}) (Strobel & Russell, 1989). Cellular ATP was assayed by extracting cells with perchloric acid, neutralizing with KOH and K_2CO_3 , and measuring luminescence using a luciferin-luciferase assay kit (Sigma) as previously described (Russell & Strobel, 1990).

RESULTS

Glucose-energized cells

When *S. bovis* cells were washed and incubated in buffer containing less than 0.5 mM K^+ or Na^+ , the glucose consumption rate averaged $23 \text{ mmol (g protein}^{-1} \text{ h}^{-1}$) (Fig. 1), the cells produced lactate as the sole fermentation end product, and the calculated rate of ATP hydrolysis was $46 \text{ mmol ATP (g protein}^{-1} \text{ h}^{-1}$). Addition of potassium caused cells to dramatically increase their intracellular potassium (from 20 to 400 mM), but potassium did not affect the rate of glucose consumption. Sodium additions also had no effect. The potassium uniporter valinomycin had no impact on cells incubated in buffer lacking potassium, but valinomycin doubled the glucose consumption rate when extracellular pot-

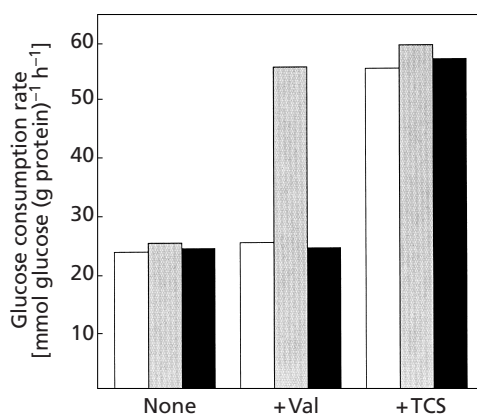


Fig. 1. Rates of glucose consumption by non-growing *S. bovis* cells with no added sodium or potassium (open bars), 5 mM potassium (grey bars) or 5 mM sodium (black bars). Cells were also treated with 1 μ M valinomycin (+Val) or 1 μ M TCS (+TCS). The sodium and potassium concentrations before addition were <0.5 mM.

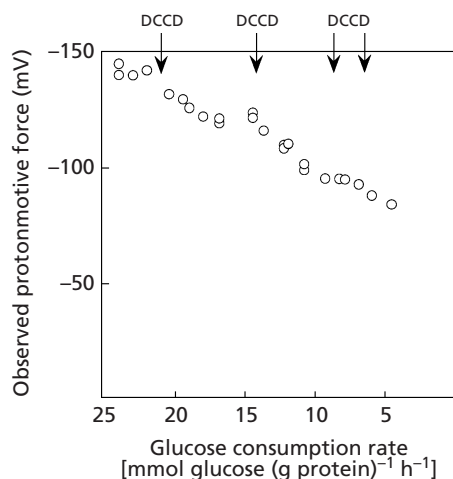


Fig. 2. Protonmotive force and glucose consumption rate of non-growing *S. bovis* cells exposed to increasing concentrations of the ATPase inhibitor DCCD. Each arrow represents an the addition of 25 μ M DCCD. Membrane potential and pH gradients for calculation of total protonmotive force were determined using distribution of [³H]TPP⁺ and [¹⁴C]benzoate, respectively.

assium was present (5 mM). Sodium additions had no effect, even if valinomycin was added (Fig. 1). TCS, a protonophore, doubled the glucose consumption and ATP hydrolysis rate under all conditions. Glucose consumption by non-growing cells decreased when small amounts of DCCD (25 μ M) were added, and larger amounts of DCCD (100 μ M) inhibited 85% of the glucose consumption rate (Fig. 2). Protonmotive force declined as glucose consumption was inhibited with DCCD, but cells treated with 100 μ M DCCD maintained a protonmotive force of approximately -80 mV.

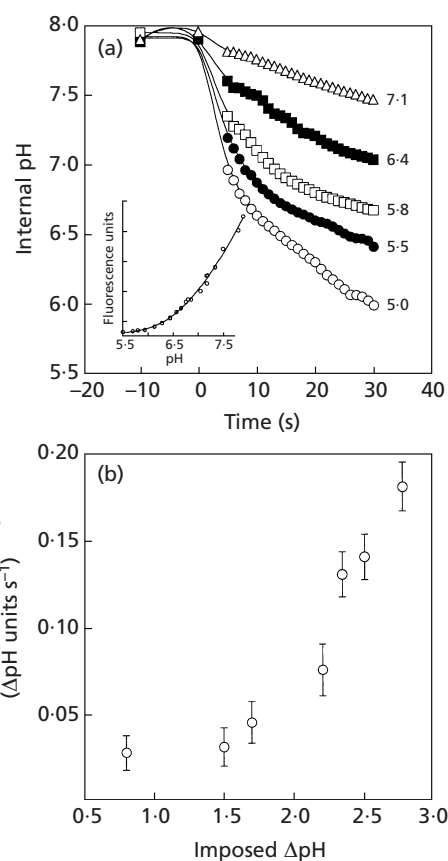


Fig. 3. (a) Internal pH of de-energized *S. bovis* cells that were shifted from pH 7.9 to lower pH values (indicated on the right of the graph) as measured with the intracellular pH probe BCECF. A sample calibration curve for BCECF in whole cells is shown inset. (b) Relationship between the initial rate of pH decline and magnitude of imposed pH gradient.

Proton flux due to artificial potentials

When cell suspensions were de-energized in pH 7.9 potassium phosphate buffer for 12 h, the internal pH was 7.8 (Fig. 3a). Pulse doses of HCl rapidly decreased the extracellular pH, and these decreases were accompanied by proton flux across the cell membrane and decay of the internal pH. The initial rate of pH decay increased as a function of imposed Δ pH, but the relationship was not linear (Fig. 3b). Cells that were treated with DCCD behaved in a similar fashion. If cells were treated with a protonophore (TCS), the decline in internal pH was almost instantaneous.

When growing cells were washed in buffer lacking potassium and sodium, the intracellular potassium concentration remained greater than 300 mM. When diluted into buffer at 39 °C, these cells leaked potassium slowly, but rapid electrogenic potassium efflux could be facilitated by valinomycin addition. When the valinomycin concentration was low (1 nM), the observed membrane potential caused by potassium efflux was only -90 mV (Fig. 4). The membrane potential in-

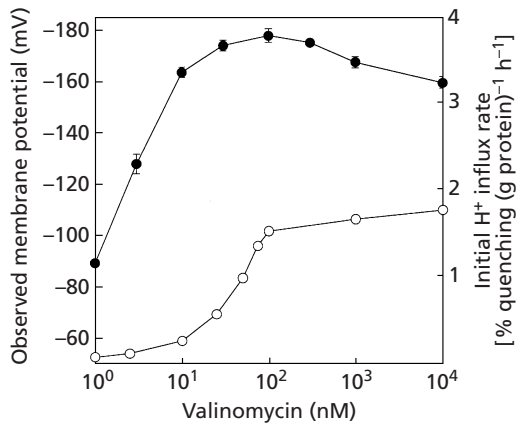


Fig. 4. Effect of valinomycin concentration on membrane potential (●) and initial rate of proton influx (○). The membrane potential was measured 10 s after valinomycin addition using [³H]TPP⁺, and the theoretical membrane potential based on flame photometry was $-183 \text{ mV} \{-62 \text{ mV} \times \log([\text{potassium}]_{\text{in}}/[\text{potassium}]_{\text{out}})\}$. The initial rate of proton influx was measured with 9-AA, where quenching of fluorescence reflects proton influx.

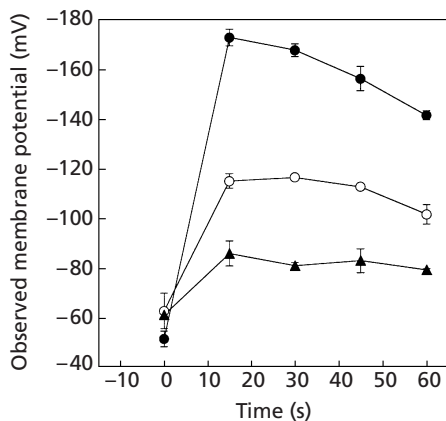


Fig. 5. Magnitude and stability of membrane potentials created by initial valinomycin-dependent potassium diffusion. The membrane potentials were varied by changing the extracellular potassium concentration. Theoretical membrane potentials based on flame photometry $\{-62 \text{ mV} \times \log([\text{potassium}]_{\text{in}}/[\text{potassium}]_{\text{out}})\}$ were -183 (●), -125 (○), and -85 (▲) mV.

creased if larger amounts of valinomycin were added, but if valinomycin concentrations were greater than 100 nM, the membrane potential decreased slightly. The membrane potential caused by valinomycin-dependent potassium efflux could be adjusted by adding external potassium, and measured values varied as predicted by the Nernst equation (Fig. 5). These potentials reached a maximum within 10 s, and decayed thereafter.

Calculations (see Discussion) indicated that a potassium efflux of only 0.025% could establish a large (-150 mV) membrane potential. Large artificial membrane

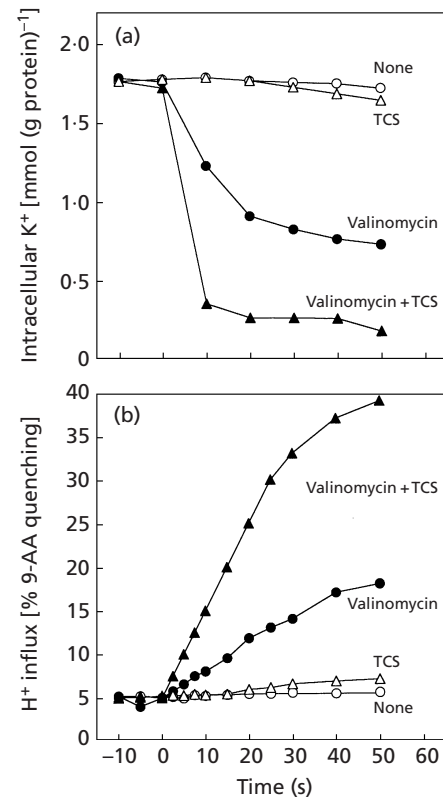


Fig. 6. (a) Intracellular potassium content of de-energized *S. bovis* cells that were treated with no ionophore (○), TCS (△), valinomycin (●) or a combination of valinomycin and TCS (▲). The theoretical membrane potential $\{-62 \text{ mV} \times \log([\text{potassium}]_{\text{in}}/[\text{potassium}]_{\text{out}})\}$ was -170 mV . (b) Proton influx as measured by 9-AA; quenching of fluorescence reflects proton influx.

potentials (negative inside) generated by valinomycin addition would prevent further potassium depletion, but the influx of other positive charges (protons) would allow additional potassium to leave. The addition of valinomycin caused rapid and very large loss ($>50\%$) of the cellular potassium (Fig. 6a), and proton influx measurements indicated that the artificial membrane potentials were causing rapid proton uptake across the cell membrane, even when a protonophore (TCS) was not present (Fig. 6b). Proton influx was valinomycin-dependent, and at least 100 nM valinomycin was needed to generate large membrane potentials and catalyse rapid proton movement across the cell membrane (Fig. 4). DCCD did not inhibit potassium efflux or proton influx, and the artificial membrane potentials did not generate ATP (data not shown).

In all cases, when cells were exposed to artificial membrane potentials, intracellular potassium decreased, intracellular proton concentrations increased, and the rate of potassium efflux was dependent on the magnitude of the artificial membrane potential. Rates based on intracellular potassium loss (cells centrifuged through silicone or trapped on filters) were higher than

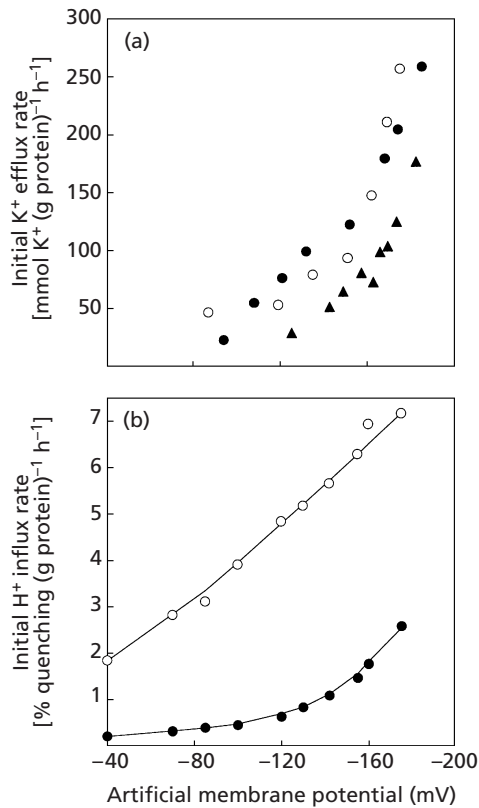


Fig. 7. (a) Relationship between artificial membrane potential and potassium efflux rate. Potassium efflux was measured by flame photometry after cells were centrifuged through silicone oil (○) or trapped on 0.45 μm filters (●). The standard error of these methods averaged $\pm 26 \text{ mmol K}^+ (\text{mg protein})^{-1} \text{ h}^{-1}$. Potassium efflux was also measured via fluorescence of CD222, an extracellular potassium-sensitive compound (▲), which had a mean standard error of $\pm 44 \text{ mmol K}^+ (\text{mg protein})^{-1} \text{ h}^{-1}$. (b) Initial rates of proton influx in response to the artificial membrane potential with (○) and without TCS (●) as measured by 9-AA; quenching of fluorescence reflects proton influx. Each point represents a duplicate determination.

efflux rates based on CD222, an extracellular potassium-sensitive compound, but the relationship between membrane potential and potassium efflux was always non-linear (Fig. 7a). The relationship between membrane potential and proton flux across the cell membrane, as measured with 9-AA, also was not linear (Fig. 7b). However, if cells were treated with TCS to facilitate proton movement, the relationship between driving force (membrane potential) and proton influx rate became nearly linear.

Inverted membrane vesicles

When intact, non-growing cells were treated with DCCD, the rate of glucose consumption and ATP hydrolysis decreased 85% [46 to 7 $\text{mmol ATP} (\text{g protein})^{-1} \text{ h}^{-1}$]. Based on a stoichiometry of 4 H^+ per ATP, the rate of proton flux across the cell membrane would have been approximately 160 $\text{mmol H}^+ (\text{g protein})^{-1} \text{ h}^{-1}$. The DCCD-sensitive ATP hydrolysis rate of

inverted membrane vesicles was faster than that in intact cells [estimated proton flux rate of 356 $\text{mmol H}^+ (\text{g vesicle protein})^{-1} \text{ h}^{-1}$], but these values were based on protein alone rather than volume. By using a ratio of cytoplasmic volume to membrane protein of 6.6 to 1 (Maloney, 1987; Cramer & Knaff, 1991), it was possible to normalize the rates for vesicles and intact cells. These calculations indicated that inverted membrane vesicles were not as active as whole cells, but the estimated rate of proton flux was still 53 $\text{mmol H}^+ (\text{g protein})^{-1} \text{ h}^{-1}$.

DISCUSSION

In *Escherichia coli*, non-growth energy consumption can be triggered by potassium deprivation, and this consumption has been explained by futile cycling of potassium ions across the cell membrane (Tempest & Neijssel, 1984; Mulder *et al.*, 1986). However, rates of potassium turnover reported by Bakker & Harold (1980) in enterococci were insufficient to explain non-growth ATP consumption, and washed *S. bovis* cells consumed glucose at a rapid rate even if potassium was not available. These results indicated that the non-growth energy dissipation of *S. bovis* was not potassium-dependent (Fig. 1).

Otto (1984) noted that *L. lactis* had a potential futile cycle of glycolytic enzymes, but this cycle only accounted for 1.5% of the glycolytic rate. Harold & Baarda (1969), Maloney (1977) and Maloney & Hanson (1982) found that ATP turnover in enterococci and lactococci could be strongly inhibited by DCCD, an inhibitor of membrane F-ATPases, and Maloney (1977) noted that this ATP consumption could also be stimulated by a protonophore. Previous work indicated that ATP dissipation in *S. bovis* cells was stimulated by TCS (a protonophore) and inhibited by DCCD (Russell & Strobel, 1990), and similar results were noted in our initial experiments (Figs 1 and 2). Inverted *S. bovis* membrane vesicles hydrolysed ATP at a rapid rate [equivalent to 13 $\text{mmol H}^+ (\text{g protein})^{-1} \text{ h}^{-1}$], and virtually all of this activity was DCCD sensitive. These observations supported the idea that that proton-pumping, membrane-bound ATPase activity was the dominant mechanism of non-growth ATP hydrolysis in *S. bovis*.

Because ATP hydrolysis is the energy source for proton-motive force generation in streptococci (Harold & Papineau, 1972), ATP hydrolysis is inhibited as the two forces approach equilibrium ($\Delta p = \Delta G^0$ of ATP hydrolysis/ n , where n is the ratio of protons pumped/ATP) (Hirata *et al.*, 1986; Van Walraven *et al.*, 1996). In order for ATP hydrolysis to continue, proton-motive force must continually be dissipated via proton conductance across the cell membrane. Reported values of 'passive' proton conductance in Gram-positive species are less than 1 $\text{mmol H}^+ (\text{g protein})^{-1} \text{ h}^{-1}$ (Maloney, 1979; Rius & Lorén, 1998; Rius *et al.*, 1994; Bender *et al.*, 1986). However, *S. bovis* had an ATP hydrolysis rate of 39 $\text{mmol ATP} (\text{g protein})^{-1} \text{ h}^{-1}$, and based on a ratio of protons pumped/ATP of 4, the proton conductance of *S. bovis* was 156 $\text{mmol H}^+ (\text{g protein})^{-1} \text{ h}^{-1}$, a value

150-fold greater than previously measured values. The protonmotive force of glycolysing *S. bovis* cells was approximately -150 mV, but proton conductance values in other bacteria were estimated at much lower driving forces (approx. -6 mV). Ohm's law states that current (proton flux) increases as a linear function of driving force (mV), but even this correction could not explain the estimated membrane conductance of *S. bovis* cells.

Rapid pH shifts are a straightforward method for generating large protonmotive forces, and a variety of workers have used this technique to estimate proton flux in liposomes (Deamer & Nichols, 1989). Converting rates of pH change to rates of proton flux is dependent on an estimate of cellular buffering capacity, and while literature values for lactic acid bacteria average approximately 200 nmol H^+ (mg protein) $^{-1}$ per pH unit over an internal pH of 7 to 8, values vary from 50 to at least 350 nmol H^+ (mg protein) $^{-1}$ per pH unit (Maloney, 1979; Rius *et al.*, 1994; Rius & Lorén, 1998). When *S. bovis* cells were subjected to a pH gradient of 2.75 pH units (-170 mV), the internal pH declined at a rate of 0.15 pH units s^{-1} , and based on a buffering capacity estimate of 200 nmol H^+ (mg protein) $^{-1}$ per pH unit, proton conductance was 108 mmol H^+ (g protein) $^{-1} h^{-1}$. As the magnitude of the pH gradient was decreased, the initial rate of proton conductance declined in a non-ohmic fashion, to an estimated rate of 10 mmol H^+ (g protein) $^{-1} h^{-1}$ at a Δ pH of 0.75 (-46 mV). These rates were much faster than previously measured values of proton conductance in similar bacteria.

Electrogenic potassium diffusion is also a common method of generating large membrane potentials, because large potassium efflux can only occur if other ions (e.g. protons) enter the cell. For instance, when *S. bovis* cells were loaded with 300 mM potassium, each cell had approximately 12×10^7 internal potassium ions, and over 98% of this potassium was free (Strobel & Russell, 1989). Based on a membrane capacitance of $1 \mu F cm^{-2}$, an efflux of only 30000 potassium ions per cell ($<0.025\%$ of the total potassium) would have generated a membrane potential of -150 mV (Maloney, 1987; Cramer & Knaff, 1991). Because valinomycin-treated cells lost more than 50% of their intracellular potassium in a very short time, it appeared that influx of another ion was allowing potassium loss. 9-AA measurements indicated that valinomycin-treated cells took up protons at a rapid rate, but these measurements were not quantitative.

Maloney (1977) used extracellular pH measurements to estimate proton fluxes in dense suspensions of *L. lactis* cells, and noted that potassium efflux via valinomycin was balanced by a stoichiometric (1:1) influx of protons. The idea that potassium efflux was coupled with proton influx was also supported by the observation that TCS greatly increased the rate of potassium efflux and proton influx. Because membrane potentials were always below the threshold required for proton influx via the ATPase (as evidenced by the lack of an effect of DCCD and the

data of Maloney, 1977), potassium movements provided an estimate of proton conductance across the cell membrane. Regardless of the method used, potassium efflux measurements demonstrated that proton influx was a non-ohmic function of imposed membrane potential, and rates were always in excess of previously reported values.

Proton conductance is often expressed in terms of membrane surface area. *S. bovis* has a mean cell composition of 50% protein and 10% lipid by weight (Russell & Robinson, 1984), and Brookes *et al.* (1997) estimated that lipid bilayers have 2200 cm 2 of surface area per mg lipid. Based on this relationship [440 cm 2 (mg protein) $^{-1}$] a proton leak rate of 100 mmol H^+ (g protein) $^{-1} h^{-1}$ of *S. bovis* corresponds to 6.2×10^{-11} mol H^+ (cm membrane) $^{-2} s^{-1}$. Respiring liver mitochondria have proton leak rates that range from 0.8 to 3.6×10^{-11} mol H^+ (cm membrane) $^{-2} s^{-1}$ and these leak rates are also non-ohmic (Krishnamoorthy & Hinkle, 1984; Brookes *et al.*, 1997; Brand *et al.*, 1994).

Other lactic acid bacteria had non-growth ATP hydrolysis at rates comparable to those estimated for *S. bovis* (Rosenberger & Elsdén, 1960; Fordyce *et al.*, 1984), but direct measurements of proton conductance could not explain these high rates of ATP turnover (Maloney, 1979; Rius & Lorén, 1998; Rius *et al.*, 1994; Bender *et al.*, 1986). These discrepancies can be explained by the non-ohmic relationship between proton conductance and driving force. When the driving force was low (<40 mV), the proton conductance of *S. bovis* was similar to the values previously reported. However, if the driving force was similar to ones found in glycolysing cells (160 mV), the proton conductance was at least 10-fold higher. Further work is needed to define the nature of this proton-conducting pathway.

ACKNOWLEDGEMENTS

This research was supported by the US Dairy Forage Research Center.

REFERENCES

- Bakker, E. P. & Harold, F. M. (1980). Energy coupling to potassium transport in *Streptococcus faecalis*. *J Biol Chem* **255**, 433–440.
- Bender, G. R., Sutton, S. V. W. & Marquis, R. E. (1986). Acid tolerance, proton permeabilities, and membrane ATPases of oral streptococci. *Infect Immun* **53**, 331–338.
- Bond, D. R. & Russell, J. B. (1996). A role for fructose 1,6-diphosphate in the ATPase-mediated energy-spilling reaction of *Streptococcus bovis*. *Appl Environ Microbiol* **62**, 2095–2099.
- Bond, D. R. & Russell, J. B. (1998). Relationship between intracellular phosphate, proton motive force, and rate of nongrowth energy dissipation (energy spilling) in *Streptococcus bovis* JB1. *Appl Environ Microbiol* **64**, 976–981.
- Brand, M. D., Chien, L.-F., Ainscow, E. K., Rolfe, D. F. S. & Porter, R. K. (1994). The causes and functions of mitochondrial proton leak. *Biochim Biophys Acta* **1187**, 132–139.
- Brookes, P. S., Rolfe, D. F. S. & Brand, M. D. (1997). The proton permeability of liposomes made from mitochondrial inner

- membrane phospholipids: comparison with isolated mitochondria. *J Membr Biol* **155**, 167–174.
- Casadio, R., Di Bernardo, S., Fariselli, P. & Melandri, A. (1995).** Characterization of 9-aminoacridine interaction with chromatophore membranes and modelling of the probe response to artificially induced transmembrane pH gradients. *Biochim Biophys Acta* **1237**, 23–30.
- Cramer, W. A. & Knaff, D. B. (1991).** *Energy Transduction in Biological Membranes. A Textbook of Bioenergetics*, p. 103. New York: Springer.
- Deamer, D. W. & Nichols, J. W. (1989).** Proton flux in model and biological membranes. *J Membr Biol* **107**, 91–103.
- Fordyce, A. M., Crow, L. & Thomas, T. D. (1984).** Regulation of product formation during glucose or lactose limitation in nongrowing cells of *Streptococcus lactis*. *Appl Environ Microbiol* **483**, 332–337.
- Harold, F. M. & Baarda, J. R. (1969).** Inhibition of membrane-bound adenosine triphosphatase and of cation transport in *Streptococcus faecalis* by *N,N'*-dicyclohexylcarbodiimide. *J Biol Chem* **244**, 2261–2268.
- Harold, F. M. & Papineau, P. (1972).** Cation transport and electrogenesis by *Streptococcus faecalis*. I. The membrane potential. *J Membr Biol* **8**, 27–44.
- Hirata, H., Ohno, K., Sone, N., Kagawa, Y. & Hamamoto, T. (1986).** Direct measurement of the electrogenicity of the H⁺-ATPase from thermophilic bacterium PS3 reconstituted in planar phospholipid bilayers. *J Biol Chem* **261**, 9839–9843.
- Krishnamoorthy, G. & Hinkle, P. C. (1984).** Non-ohmic proton conductance of mitochondria and liposomes. *Biochemistry* **23**, 1640–1645.
- Lolkema, J. S., Helligwerf, K. J. & Konings, W. N. (1982).** The effect of 'probe binding' on the quantitative determination of the proton-motive force in bacteria. *Biochim Biophys Acta* **1681**, 85–94.
- Maloney, P. C. (1977).** Obligatory coupling between proton entry and the synthesis of adenosine 5'-triphosphate in *Streptococcus lactis*. *J Bacteriol* **132**, 564–575.
- Maloney, P. C. (1979).** Membrane H⁺ conductance of *Streptococcus lactis*. *J Bacteriol* **140**, 197–205.
- Maloney, P. C. (1987).** In *Escherichia coli and Salmonella typhimurium: Cellular and Molecular Biology*, vol. 1, pp. 223–225. Edited by F. C. Neidart and others. Washington, DC: American Society for Microbiology.
- Maloney, P. C. & Hansen, F. C. (1982).** Stoichiometry of proton movements coupled to ATP synthesis driven by a pH gradient in *Streptococcus lactis*. *J Membr Biol* **66**, 63–75.
- Molenaar, D., Abee, T. & Konings, W. N. (1991).** Continuous measurement of the cytoplasmic pH in *Lactococcus lactis* with a fluorescent pH indicator. *Biochim Biophys Acta* **115**, 75–83.
- Molenaar, D., Bolhuis, H., Abee, T., Poolman, B. & Konings, W. N. (1992).** The efflux of a fluorescent probe is catalyzed by an ATP-driven extrusion system in *Lactococcus lactis*. *J Bacteriol* **174**, 3118–3124.
- Mulder, M. M., Teixeira de Mattos, M. J., Postma, P. W. & van Dam, K. (1986).** Energetic consequences of multiple K⁺ uptake systems in *Escherichia coli*. *Biochim Biophys Acta* **851**, 223–228.
- Neijssel, O. M. & Teixeira de Mattos, M. J. (1994).** The energetics of bacterial growth: a reassessment. *Mol Microbiol* **13**, 179–182.
- Otto, R. (1984).** Uncoupling of growth and acid production in *Streptococcus cremoris*. *Arch Microbiol* **140**, 225–230.
- Rius, N. & Lorén, J.-G. (1998).** Buffering capacity and membrane H⁺ conductance of neutrophilic and alkaliphilic gram-positive bacteria. *Appl Environ Microbiol* **64**, 1344–1349.
- Rius, N., Solé, M., Francia, A. & Lorén, J.-G. (1994).** Buffering capacity and membrane H⁺ conductance of lactic acid bacteria. *FEMS Microbiol Lett* **120**, 291–296.
- Rosenberger, R. F. & Elsdén, S. R. (1960).** The yields of *Streptococcus faecalis* grown in continuous culture. *J Gen Microbiol* **22**, 726–739.
- Russell, J. B. & Cook, G. M. (1995).** Energetics of bacterial growth: balance of anabolic and catabolic reactions. *Microbiol Rev* **59**, 48–62.
- Russell, J. B. & Robinson, P. H. (1984).** Compositions and characteristics of strains of *Streptococcus bovis*. *J Dairy Sci* **67**, 1525–1531.
- Russell, J. B. & Strobel, H. J. (1990).** ATPase-dependent energy spilling by the ruminal bacterium *Streptococcus bovis*. *Arch Microbiol* **153**, 378–383.
- Russell, J. B., Strobel, H. J., Driessen, A. J. M. & Konings, W. N. (1988).** Sodium-dependent transport of neutral amino acids by cells and membrane vesicles of *Streptococcus bovis*, a ruminal bacterium. *J Bacteriol* **170**, 3531–3536.
- Strobel, H. J. & Russell, J. B. (1989).** Non-proton-motive-force-dependent sodium efflux from the ruminal bacterium *Streptococcus bovis*: bound versus free pools. *Appl Environ Microbiol* **55**, 2664–2668.
- Tempest, D. W. & Neijssel, O. M. (1984).** The status of Y_{ATP} and maintenance energy as biologically interpretable phenomena. *Annu Rev Microbiol* **38**, 459–486.
- Taylor, M. A. & Jackson, J. B. (1987).** Adaptive changes in membrane conductance in response to changes in specific growth rate in continuous cultures of phototrophic bacteria under conditions of energy sufficiency. *Biochim Biophys Acta* **891**, 242–255.
- Van Walraven, H. S., Heinrich, S., Schwartz, O. & Rumberg, B. (1996).** The H⁺/ATP coupling ratio from thiol-modulated chloroplasts and two cyanobacterial strains is four. *FEBS Lett* **379**, 309–313.

Received 23 August 1999; revised 11 November 1999; accepted 2 December 1999.